Wave scattering from multiple circular floating porous elastic plates

Siming Zheng[a]†, **Michael H. Meylan**[b], **Guixun Zhu**[a], **Deborah Greaves**[a], **Gregorio Iglesias**[c,a]

a. School of Engineering, Computing and Mathematics, University of Plymouth, Drake Circus, Plymouth PL4 8AA, UK
b. School of Mathematical and Physical Sciences, The University of Newcastle, Callaghan 2308, Australia
c. MaREI, Environmental Research Institute and School of Engineering, University College Cork, Ireland
† Email: siming.zheng@plymouth.ac.uk

1. Introduction

Among the wide variety of nearshore and offshore artificial structures, some might be identified as floating porous elastic plates with small draught relative to their horizontal dimensions, e.g., floating flexible breakwaters, artificial floating vegetation fields and extensive aquaculture farms. Therefore, it is essential to study the flexural deformations of floating porous elastic plates subjected to water waves and to evaluate the wave dissipation caused by their porosity.

Water-wave interaction with floating elastic plates has been widely studied, most of these plates were non-porous [1-5]. Less research work for porous elastic plates has been reported, except the investigation carried out by Meylan et al. (2017), Koley et al. (2018) and Zheng et al. (2020), which were focused on a single porous elastic plate [6-8]. For an array of such porous elastic plates, especially with the individual plates deployed close to each other, the hydrodynamic interaction between them can significantly influence their responses. In this paper, a theoretical model is developed based on linear potential flow theory and an eigenfunction matching method to investigate wave scattering by multiple circular floating porous elastic plates with three different types of edge conditions, i.e., free -, simply supported -, and clamped edges. Two methods for evaluating the exact power dissipated by the array of porous plates are proposed.

2. Mathematical model

Consider N circular porous elastic plates floating in water of finite depth h (see Fig.1, $N=2$ is taken as an example), N local cylindrical coordinates $O_n r_n \theta_n z$ are defined with their origins O_n located on the central vertical axis of the n-th plate. A Cartesian coordinate system $Oxyz$ is applied to describe the wave scattering problem with $z=0$ at the mean water surface and Oz pointing upwards. Additionally, one more cylindrical coordinate system $Or_0 \theta_0 z$ is defined with its origin coinciding with the Cartesian coordinate system (not plotted in Fig. 1). The mean wetted surface of the n-th plate is denoted as Ω_n. The radius of the n-th plate is denoted by R_n. β denotes the incident wave direction. R_{jn} and α_{jn} are the norm and the angle of vector $O_j O_n$. The water domain is divided into two types, a) interior region, i.e., the region beneath each plate, and b) exterior region, i.e., the rest extending towards infinite distance horizontally.
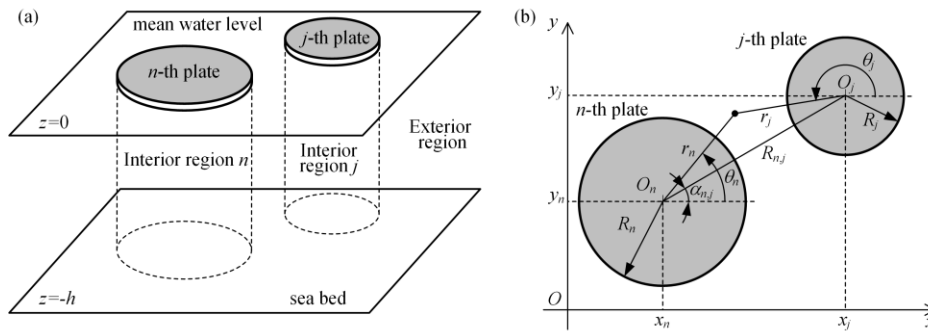

Fig. 1. Definition sketch: (a) bird view; (b) top view.

Within the framework of linear potential flow theory, the fluid flow in the water domain can be described by the velocity potential φ, which satisfies the Laplace equation, the boundary conditions at sea bed and the water surface of the exterior region, and the kinematic and dynamic conditions at Ω_n ($n=1, 2, .., N$) [6]

$$\partial_z \varphi = -\mathrm{i}\omega\eta^{(n)} + \mathrm{i}P\varphi, \quad g\left[\chi\Delta^2 + 1 - \left(\omega^2/g\right)\gamma\right]\eta^{(n)} - \mathrm{i}\omega\varphi = 0, \tag{1}$$

where ω is the angular wave frequency; $\eta^{(n)}$ denotes the complex vertical displacement of the lower surface of the n-th plate; P is the porosity parameter; g is the gravitational acceleration; γ and χ denote the mass per unit area and the

flexural rigidity of the plate, respectively, scaled with respect to the water density; P, χ, and γ can be non-dimensionalised with respect to the water depth as $\bar{P}=Ph$, $\bar{\chi}=\chi/h^4$ and $\bar{\gamma}=\gamma/h$. Δ is the Laplacian operator in the horizontal plane.

In different subdomains, the velocity potential φ can be expressed as follows:

(1) Exterior domain

$$\varphi_{\text{ext}}\left(r_n,\theta_n,z\right)=\varphi_1+\sum_{m=0}^{\infty}\sum_{l=0}^{\infty}A_{m,l}^{(n)}H_m\left(k_l r_n\right)Z_l\left(z\right)e^{im\theta_n}$$
$$+\sum_{\substack{j=1\\j\neq n}}^{N}\sum_{m=0}^{\infty}\sum_{l=0}^{\infty}A_{m,l}^{(j)}Z_l\left(z\right)\sum_{m'=-\infty}^{\infty}\left(-1\right)^{m'}H_{m-m'}\left(k_l R_{n,j}\right)J_{m'}\left(k_l r_n\right)e^{i\left(m\alpha_{j,n}+m'\alpha_{n,j}\right)}e^{im'\theta_n}\quad,R_n<R_{jn}\tag{2}$$

(2) Interior domain [6]

$$\varphi_{\text{int}}\left(r_n,\theta_n,z\right)=\sum_{m=-\infty}^{\infty}\sum_{l=-2}^{\infty}B_{m,l}^{(n)}J_m\left(\kappa_l r_n\right)Y_l\left(z\right)e^{im\theta_n}\ ,\tag{3}$$

where

$$Z_l\left(z\right)=\frac{\cosh\left[k_l\left(z+h\right)\right]}{\cosh\left(k_l h\right)},\ l=1,2,\ldots;\ \ Y_l\left(z\right)=\frac{\cosh\left[\kappa_l\left(z+h\right)\right]}{\cosh\left(\kappa_l h\right)},\quad l=-2,-1,0,1,2,\ldots\tag{4}$$

$A_{m,l}^{(n)}$, and $B_{m,l}^{(n)}$ are the unknown coefficients to be solved; k_l ($l=0,1,2,\ldots$) and κ_l ($l=-2,-1,0,1,2,\ldots$) are the roots of the dispersion relations for the exterior- and interior domains, i.e.,

$$\omega^2=gk\tanh\left(k_l h\right)\ \ \text{and}\ \ \left[\chi\kappa_l^4+1-\left(\omega^2/g\right)\gamma\right]\left[\kappa_l\tanh\left(\kappa_l h\right)-iP\right]=\omega^2/g\ ,\tag{5}$$

respectively, in which the second dispersion relation can be derived from Eq. (1); J_m and H_m denote the Bessel function and the Hankel function of the first kind, respectively. The pressure and velocity continuity conditions on the interfaces of each two adjacent regions, together with the free -, simply supported -, or clamped edge conditions are used to solve the unknown coefficients.

The energy dissipated by the N plates due to porosity can be calculated by a straightforward method

$$P_{\text{diss}}=\frac{\rho\omega P}{2}\sum_{n=1}^{N}\iint_{\Omega_n}\left|\varphi\right|^2\,ds=\frac{\rho\omega P}{2}\sum_{n=1}^{N}\iint_{\Omega_n}\left|\sum_{m=-\infty}^{\infty}\sum_{l=-2}^{\infty}B_{m,l}^{(n)}J_m\left(\kappa_l r_n\right)e^{im\theta_n}\right|^2\,ds\ .\tag{6}$$

An indirect method based on Kochin function provides an alternative way to evaluate P_{diss}

$$P_{\text{diss}}=\frac{\rho\omega\tanh\left(kh\right)}{k}\left[1+\frac{2kh}{\sinh\left(2kh\right)}\right]\left(\frac{Ag}{2\omega}\text{Re}\left[H_R\left(\beta\right)\right]-\frac{1}{8\pi}\int_0^{2\pi}\left|H_R\left(\theta_0\right)\right|^2\,d\theta_0\right),\tag{7}$$

where H_R is the Kochin function

$$H_R\left(\theta_0\right)=2\sum_{n=1}^{N}\sum_{m=-\infty}^{\infty}A_{m,0}^{(0)}e^{-ikR_{0,n}\cos\left(\alpha_{0,n}-\theta_0\right)}\left(-i\right)^{m+1}e^{im\theta_0}\ .\tag{8}$$

3. Results and discussions

Montiel et al. (2013) carried out a series of wave basin experiments of a pair of elastic circular plates and observed strong hydrodynamic interaction between them [3]. Figure 2 illustrates the theoretical and experimental deflection of four markers on each plate. It is shown that the present conceptual model can be used to predict the response of the two elastic plates well, and it gives insights on how the two plates affect each other's response.
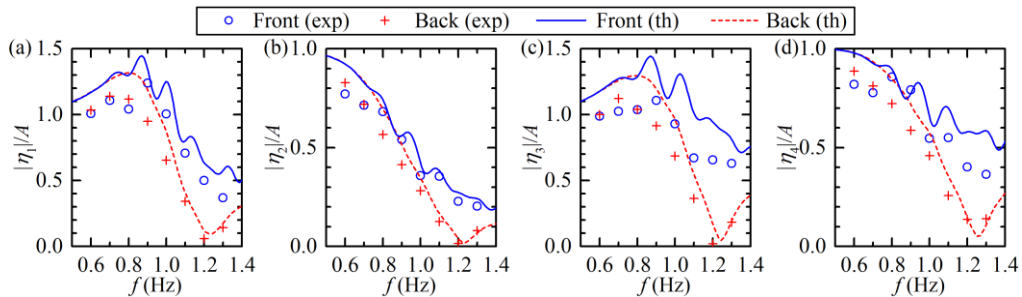

Fig. 2. Deflection of (a) marker 1 ($r_n=R_n$, $\theta_n=0$); (b) marker 2 ($r_n=0$); (c) marker 3 ($r_n=R_n$, $\theta_n=\pi$) and (d) marker 4 ($r_n=R_n$,

$\theta_n = \pi/2$) for the two-plates as a function of frequency. Each figure contains the present theoretical results and the experimental data [3] associated with both plates. [$R_1=R_2=0.72$ m, $h=1.9$ m, $R_{12}=x_2-x_1=3.0$ m, $y_1=y_2=0$, $\beta=\pi$, $P=0$, $\bar{\chi}=3.55\times10^{-4}$, $\bar{\gamma}=2.79\times10^{-3}$, free edge].

Wave power dissipation by two porous elastic plates are evaluated by using both the direct- and indirect methods, the results of which are illustrated in Fig. 3, where P_{diss} is non-dimensionalised as $\eta_{diss}=kP_{diss}/P_{in}$ with k the wave number and P_{in} the incident wave power per unit width of the wave front. The excellent agreement of the results, as shown in Fig. 3, together with those plotted in Fig. 2 gives confidence in the present theoretical model for solving wave scattering and evaluating wave dissipation by an array of circular floating porous elastic plates.
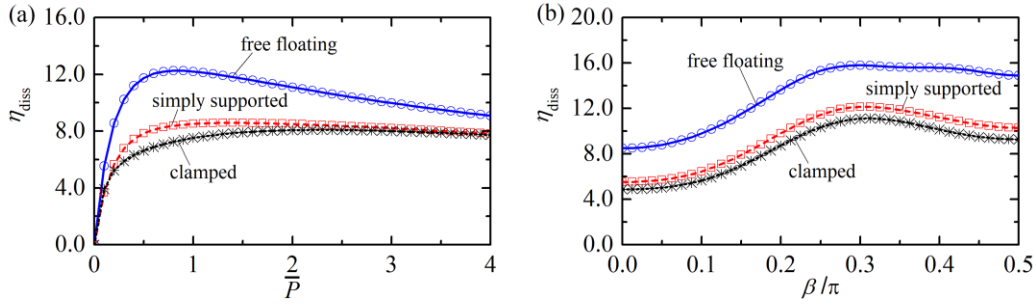

Fig. 3. Wave power dissipation of two plates with different edge conditions evaluated by using direct method (lines) and indirect method (symbols): (a) variation of η_{diss} with $\bar{P}$ for $\beta=\pi/6$; (b) variation of η_{diss} with β for $\bar{P}=1.0$. [$-x_1/h=x_2/h=3.0$, $y_1=y_2=0$, $R_1/h=R_2/h=2.0$, $h\backslash\omega^2/g=2.0$, $\bar{\chi}=\bar{\gamma}=0.01$].

Figure 4 presents how η_{diss} vary with the incident wave direction β and also with the porosity parameter $\bar{P}$ for a pair of plates deployed along the x-axis with a free floating edge, simply supported edge and clamped edge. For any specific wave incident direction, the optimal $\bar{P}$ for the free floating case is the least among the three studied cases, and the optimal $\bar{P}$ for the clamped example is the largest. Although η_{diss} varies dramatically with the change of $\bar{P}$ for $\bar{P}<0.5$ for all the three cases, it is not sensitive to $\bar{P}$ when $\bar{P}>1.0$, especially for the simply supported and clamped edge cases. For the pair of plates with a fixed porosity, the wave power dissipated by them is the smallest when incident waves propagate along the two plates, i.e., $\beta=0$. This minimal case results from the significant reduction of the wave power dissipated by the leeward plate due to the "shadowing effect" of the plate at the waveward side. The largest wave power dissipations in terms of η_{diss} for the three-edge cases are 15.79, 12.24, and 11.63, occurring at ($\bar{P}$, β/π) = (1.05, 0.30), (1.35, 0.31), and (2.10, 0.32), respectively.

Figure 5 illustrates the effect of $\bar{P}$ and $R_{1,2}/h$ on η_{diss}. In the computed range of $\bar{P}$ and $R_{1,2}/h$, there are two peaks of η_{diss} observed, one occurring at $R_{1,2}/h = 5.0$, and the other at $R_{1,2}/h = 8.0$, in which the former one is higher than the aft one, regardless of the types of the plate edge. More specifically, the largest values of η_{diss} are 16.49, 12.79, 12.38, for the free floating-, simply supported-, and clamped cases, occurring at ($\bar{P}$, $R_{1,2}/h$) =(1.25, 5.0), (2.25, 5.0) and (3.00, 5.0), respectively, which are induced by the hydrodynamic interaction between the plates, or the so-called array effect.

Figure 6 presents the variation of the wave power dissipation of an array of porous elastic plates in terms of η_{diss}/N with $\bar{P}$. For $\bar{P}<0.25$, the curves of η_{diss}/N with different values of N nearly overlap with each other, denoting the negligible impact of the plate number in the array on wave power dissipation. For the rest computed range of $\bar{P}$, i.e., $\bar{P}>0.25$, the η_{diss}/N-$\bar{P}$ curve rises with the increase of N. The most significant improvement of η_{diss}/N occurs when N increases from 1 to 2. As N turns larger and larger, the increment of η_{diss}/N gets weaker and weaker. These apply to all the edge conditions, i.e., free floating-, simply supported-, and clamped edges. Take the free floating edge case with $\bar{P}=1.0$ as an example, the η_{diss}/N corresponding to $N=1\sim5$ are 7.40, 8.19, 8.45, 8.56 and 8.63, with the increasing percentage 10.7%, 3.1%, 1.3% and 0.9%, respectively. It can also be observed that the more plates the array contains, the larger the value of $\bar{P}$ is required to achieve the maximum wave power dissipation.
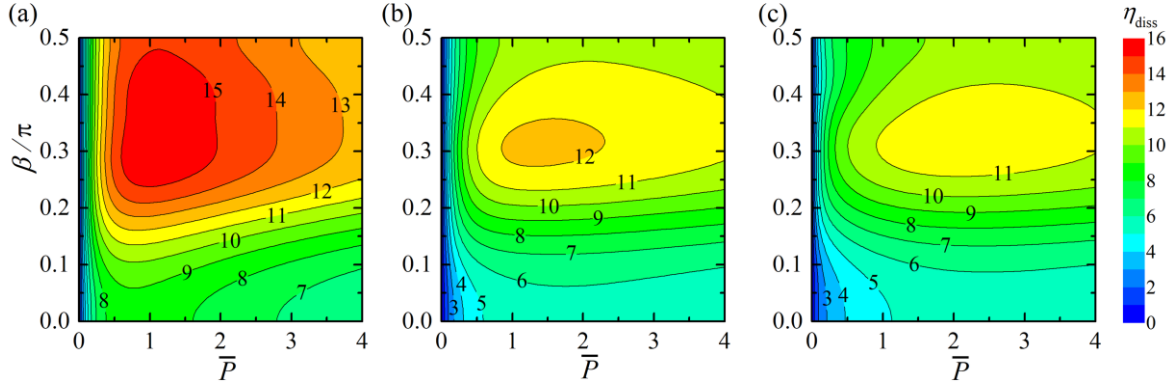
Fig. 4. Contour plot for the variation of η_{diss} as a function of $\overline{P}$ and β: (a) free floating edge; (b) simply supported edge; (c) clamped edge. [$N=2$, $-x_1/h=x_2/h=3.0$, $y_1=y_2=0$, $R_1/h=R_2/h=2$, $h\omega^2/g=2.0$, $\overline{\chi}=\overline{\gamma}=0.01$].
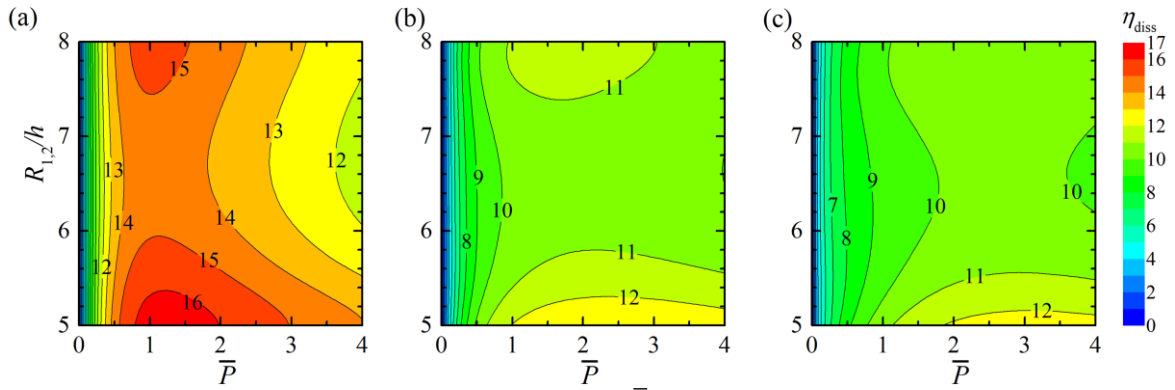

Fig. 5. Contour plot for the variation of η_{diss} as a function of $\overline{P}$ and $R_{1,2}$: (a) free floating edge; (b) simply supported edge; (c) clamped edge. [$N=2$, $-x_1/h=x_2/h=0.5R_{1,2}/h$, $y_1=y_2=0$, $R_1/h=R_2/h=2.0$, $h\omega^2/g=2.0$, $\beta=\pi/2$, $\overline{\chi}=\overline{\gamma}=0.01$].
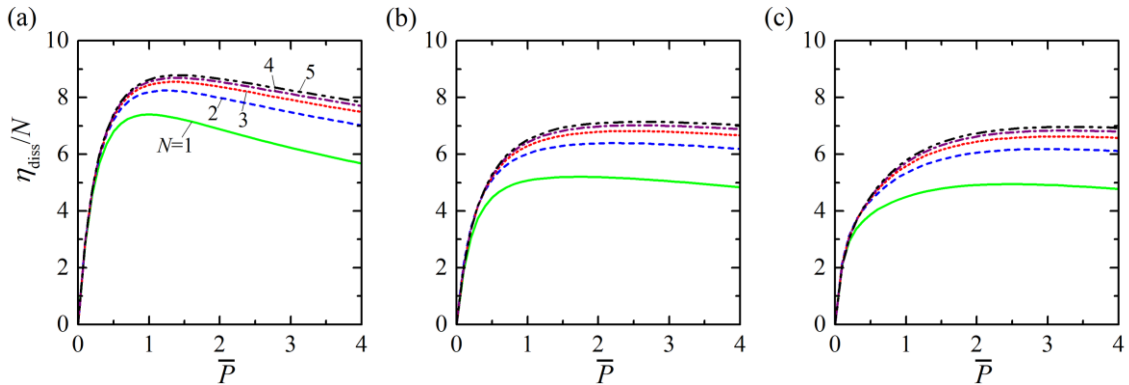

Fig. 6. Variation of η_{diss}/N with $\overline{P}$ for different number of plates in the array, N: (a) free floating edge; (b) simply supported edge; (c) clamped edge. [$(x_{j+1}-x_j)/h=5.0$, $y_j=0$, $R_1/h=R_2/h=2.0$, $h\omega^2/g=2.0$, $\beta=\pi/2$, $\overline{\chi}=\overline{\gamma}=0.01$].

References

[1]. Sahoo, T., Yip, T.L., Chwang, A.T., 2001. Scattering of surface waves by a semi-infinite floating elastic plate. Physics of Fluids. 13(11), 3215.

[2]. Porter, R., Evans, D.V., 2006. Scattering of flexural waves by multiple narrow cracks in ice sheets floating on water. Wave Motion. 43(5), 425-443.

[3]. Montiel, F., Bonnefoy, F., Ferrant, P., Bennetts, L.G., Squire, V.A., Marsault, P., 2013. Hydroelastic response of floating elastic discs to regular waves. part 1. wave basin experiments. Journal of Fluid Mechanics 723, 604–628.

[4]. Li, Z.F., Wu, G.X., Ji, C.Y., 2018. Interaction of wave with a body submerged below an ice sheet with multiple arbitrarily spaced craks. Physics of Fluids, 30(5), 057107.

[5]. Squire, V.A., 2020. Ocean wave interactions with sea ice: a reappraisal. Annual Review of Fluid Mechanics, 52, 37–60.

[6]. Meylan, M.H., Bennetts, L.G., Peter, M.A., 2017. Water-wave scattering and energy dissipation by a floating porous elastic plate in three dimensions. Wave Motion, 70, 240-250.

[7]. Koley, S., Mondal, R., Sahoo, T., 2018. Fredholm integral equation technique for hydroelastic analysis of a floating flexible porous plate. European Journal of Mechanics/B Fluids. 67, 291-305.

[8]. Zheng, S., Meylan, M.H., Fan, L., Greaves, D., Iglesias, G., 2020. Wave scattering by a floating elastic plate of arbitrary shape: A semi-analytical study. Journal of Fluids and Structures, 92, 102827.